EB-PVD TBCs of Zirconia Co-doped with Yttria and Niobia, a Microstructural Investigation

D. S. Almeida *[a], C.R.M. Silva [a], M.C.A. Nono [b], C.A.A. Cairo [a]

[a] Centro Técnico Aeroespacial – Divisão de Materiais AMR-CTA, Pça. Marechal do Ar Eduardo Gomes, 50, cep. 12228-904, S. J.Campos – SP Brazil

[b] Instituto Nacional de Pesquisas Espaciais - Laboratório Associado de Materiais e Sensores LAS-INPE, Av. dos Astronautas, 1758 cep 12227-010, S. J. Campos - SP Brazil.

Abstract: Turbine blades of airplanes and thermoelectric plants work in adverse conditions, with corrosive environment and high temperature and pressure. One way to improve the life and/or the working temperature of the blades is the use of special coatings over metallic material applied by Electron Beam – Physical Vapor Deposition (EB-PVD). The most usual material for this application is yttria doped zirconia. Addition of niobia, as a co-dopant in the Y_2O_3-ZrO_2 system, can reduce the thermal conductivity and improve mechanical properties of the coating. The purpose of this work is to show the influence of the addition of niobia on the microstructure of ceramic coatings by using x-ray diffraction (XRD) techniques and scanning electron microscopy (SEM) observations. SEM on fractured cross section shows a columnar structure and the results of XRD show only zirconia tetragonal phase in the ceramic coating for the chemical composition range studied. As the difference ($NbO_{2.5}$ - $YO_{1.5}$) mol % increases, the ratio c/a (tetragonality) increases. Considering that the t-ZrO_2 solid solutions begins unstable when the relation c/a exceeds 1.020, it is possible to evaluate the maximum niobia content that can be added to the coating without losses in its mechanical properties. SEM on ceramic coatings polished cross section shows color bands associated with chemical composition changes due to the differences in saturation vapor pressure of the individual components. As the niobia content increases, there is a tendency to reduction of the ceramic coating theoretical density.

* Corresponding author. Tel.: +55 (12) 3947 6470; FAX: +55 (12) 3947 6405

E-mail address: **dsa62@yahoo.com** (D. S. Almeida)

1. Introduction

The EB-PVD process allows attaining coverings with unique properties. The process parameters are adjusted so that the deposit has a columnar grains structure perpendicular to the interface. This morphology maximizes the resistance to strains that arise from differences in thermal expansion coefficients. Others advantages are: aerodynamically favorable smooth surface, better interaction with the substrate, greater thermal cycle tolerance and, hence, greater lifetime comparatively with the plasma spray process. [1-9].

There are four primary constituents in a thermal protection system. They comprise: (1) the thermal barrier coating (TBC) it self based usually in ~ 8 wt. % (8,7 mol % $YO_{1.5}$) yttria stabilized zirconia; (2) the metallic component, treated here as the substrate; (3) an aluminium containing bond coat (BC) located between the substrate and the TBC; and (4) a thermally grown oxide (TGO), predominantly α-alumina, that forms between the TBC and the bond coat. The TBC is the thermal insulator, the bond coat provides oxidation protection, since the zirconia is essentially transparent for the oxygen at high temperatures, and the metallic component, usually a nickel base super-alloy, sustains the structural loads. The TGO is an oxidation reaction product of the bond layer, and plays a role in the metal/oxide adhesion. Each of these elements is dynamic and all interact to control the performance and durability [10-12].

In this configuration, the system presents a gradual thermal expansion coefficients transition of the substrate (16×10^{-6}/K), passing through of the bond coating ($11–13 \times 10^{-6}$/K), and finished at the ceramic coating ($5–10 \times 10^{-6}$/K). This gradual transition reduces the thermal stresses generated during the TBCs operation [13, 14].

When ZrO_2 is utilized for technical applications the high-temperature polymorphs cubic (c) and tetragonal (t) phases should be stabilized at room temperature by the formation of solid solutions, which prevent deleterious tetragonal-to-monoclinic (m) phase transformation. The alloying oxides, which lead to the stabilization, are alkaline-earth, rare-earth, and actinide oxides. It has been suggested that the factors, which may influence the stabilization, are size, valency, and concentration of solute cations and crystal structure of the solute oxides, where the valency and concentration determine the number of oxygen vacancies created by the formation of substitutional solid solutions [15, 16].

The addition of Ta_2O_5, Nb_2O_5, and HfO_2 to bulk Y_2O_3-stabilized tetragonal ZrO_2 increases the transformability (t to m transformation temperature) of the resulting zirconia ceramics. The enhanced transformability is related to the alloying effect on the tetragonality (c/a - cell parameters ratio) of stabilized tetragonal ZrO_2 (Figure 1), so the addition of these oxides increases the tetragonal distortion of the cubic lattice. The increase in the tetragonality due to alloying is consistent with the increase in the fracture toughness and the increase in the t to m transformation temperature. Evidently, t-ZrO_2 become unstable as their tetragonality increases toward 1.020, which corresponds to the c/b axial ratio of m-ZrO_2 at room temperature. On the other hand, they become stable as the tetragonality decreases toward unity, which corresponds to c-ZrO_2. This relationship allows the classification of oxides into either a stabilizer (decreasing tetragonality) or a destabilizer (increasing tetragonality) for the t-ZrO_2 phase [15,17,18].

Thermal conductivity of bulk 6 to 8wt.% yttria partially stabilized zirconia is 2.2 to 2.9 W/mK, standards plasma sprayed zirconia coatings is typically 0.9 to 1.0 W/mK and standards EB-PVD coatings is typically 1.8 to 2.0 W/mK [19].

When a trivalent oxide, e.g. Y_2O_3, is added to ZrO_2 as stabilizer, certain amount of lattice defects, e.g. oxygen vacancies and negatively-charged solutes, are produced in the ZrO_2 lattice. The thermal conductivity of partially stabilized-ZrO_2 (PSZ) is determined by its defect structure and the defect associates between them. Pentavalent oxides are positively charged, opposite to the stabilizer, when dissolved in the ZrO_2 lattice, the addition of these oxides in the PSZ will definitely affect the original defect structure, thus also its properties. Ta_2O_5 has been found to affect the phase stability and the electrical properties of ZrO_2, and Nb_2O_5 has also been found to dramatically change the grain boundary electrical conductivity [20-22].

The effect of doping with pentavalent oxides such as tantala and niobia (cationic radii in the +5 oxidation state ~ 0.68Å for both) indicate that both ions reside as substitutional defects in the zirconium lattice (ionic radius of the Zr^{4+} ion is 0.79 Å), annihilating oxygen vacancies generated by yttria doping. Thus, the defect chemistry generated by the two dopants is also identical and would be expected to scatter phonons due to the difference in ionic radius and atomic bonding [20].

Figure 2 presents the phase diagram available for the Nb_2O_5-ZrO_2 system [23]; at temperatures in excess of 1400^oC indicate limited solubility of the pentavalent oxide in zirconia (~20 wt. % or ~ 19 mol % $NbO_{2.5}$). However, co-doping with yttria has been observed to enhance their solubility in the tetragonal phase [18, 20].

The present work analyzes the addition of niobia, as co-dopant in the yttria-zirconia coating system. The study of the considered ceramic coating is motivated by the potential of the niobia overcome the deficiencies presented in conventional yttria stabilized zirconia coatings i.e., high thermal conductivity when compared with plasma spray coatings and relatively low mechanical properties. Lowering coatings thermal conductivity would increase the engine performance by improving the combustion efficiency, reduce the specific fuel consumption, allow a reduction of internal cooling, reduce the metallic component temperature and extend their lifetime. Research in zirconia co-doped with yttria and niobia sintered tablets show low thermal conductivity and high tenacity [24, 25]. The purpose of this work is to show the influence of the addition of niobia on the microstructure of ceramic coatings.

2. Experimental

SAE 304 stainless steel plates 30 x 10 x 1.59 mm^3 were used as metallic substrates. Both bond layer and ceramic top coating were EB-PVD deposited using an one source 30 kW electron beam equipment. It consists of an electron gun with an accelerating voltage of 25 kV and beam current variation from 0 to 1.2 A. The vacuum system has an ultimate pressure of 10^{-6} torr (~ 10^{-4} Pa). A substrate holder assembly is situated above the vapor source at a vertical distance of 150 mm. A tungsten filament is used to heat the substrate by Joule effect to the desired temperature (~900^oC), which is measured and maintained by a thermocouple and programmable temperature controller. A water-cooled copper crucible is used for evaporation of sintered targets. The targets (cylinders of 20 mm diameter and mass of 20 gram) was prepared from cold compacted powder mixtures and sintered at 1700^oC under vacuum (10^{-4} Pa). The bond layer was Ni-31Cr-11Al-0.65Y alloy (wt.%) 25 μm thick. The nominal composition of the ceramic targets is given in Table I.

The coating crystalline phase was identified by x-ray diffraction using a diffractometer X'Pert Philips PW 1380/80 and a diffractometer X'Pert – MRD Philips with a PW 3050 goniometer. The ceramic coating microstructure and grain morphology were observed by SEM and the chemical composition was estimated by EDS using a LEO 435 VPI scanning electron microscope.

The bulk density is the relation between ceramic coating mass and its geometrical dimensions. The theoretical density, disrespecting pores and other defects, was calculate from the cell parameters (from XRD data) and molar concentrations (from EDS analysis), using the equation:

$$\rho = \frac{n.[\,x.A_{YO1,5} + y.A_{NbO\,2,5} + (1 - x - y).A_{ZrO\,2}\,]}{6,02\,.10^{23}.a^2.c} \qquad \text{Equation 1}$$

Where:

n – cations in unit cell (n=4 for fcc);
$A_{YO1.5}$ – yttria atomic mass (112.905);
$A_{NbO2.5}$ – niobia atomic mass (132.905);
A_{ZrO2} – zirconia atomic mass (123.22);
x and y – molar fraction of yttria and niobia, respectively;
a and c – cell parameters of t-ZrO_2 calculated from XRD data.

3. Results and Discussion

Figure 3 shows several zirconia based ceramic coated samples. Samples with high niobia content (higher than 10 mol % $NbO_{2.5}$) have a tendency to spall in the corner after the deposition cycle due to high stress concentration [11] and its worst mechanical properties. Typical microstructure of EB-PVD coating, as seen by scanning electron microscopy on fractured cross section, is shown in Figure 4. It is possible to see the metallic bond layer and the ceramic layer where the columnar structure is evident.

Figure 5 shows the x-ray diffractograms in scanning mode and Figure 6 the high angular resolution (0,0001° for 2θ) spectra for (400) region performed on the ceramic coating samples surface with different niobia contents. The (400) region was selected because it is specific of the nonequilibrium tetragonal phase (i.e. forbidden by the cubic symmetry [26]). All samples show only the zirconia tetragonal phase.

XRD techniques do not allows the identification of special textures related with XRD peaks intensity because the PVD coatings show a strong crystallographic texture and the diffraction patterns is taken normal to the substrate surface, not in the coating primary growth direction [27]. However, the x-ray diffraction techniques allow determining, with sufficient precision, the position of the peaks. The position of the peaks is correlated with crystalline cell lattice parameters and these vary strongly with the chemical composition of the films.

The chemical composition, the cell parameters deduced from diffraction patterns and the values of bulk and theoretical densities of the coatings are reproduced in Table I.

Figure 7 shows the influence of the difference ($NbO_{2.5}$ - $YO_{1.5}$) mol % in the zirconia tetragonality. The tetragonality was calculated from the (111) and the (400) peaks position of the XRD diffractograms on the surface of the zirconia based

coatings. Chemical composition was performed by EDS analysis on the ceramic coating cross section. As the difference ($NbO_{2.5}$ - $YO_{1.5}$) mol % increases, the ratio c/a (tetragonality) increases. Despite of the compositional gradients in the coatings and inaccuracy of oxides semi-quantitative analyses by EDS techniques the linear regression shows a high linear coefficient (R=0,920).

Researches with sintered tablets (bulk material) of stabilized tetragonal ZrO_2 show that becomes unstable as their tetragonality increases toward 1.020, at room temperature [15,18]. These researches agree with the present work experimental results where niobia-yttria-zirconia coatings with $NbO_{2.5}$ contenting higher than 7 mol % (c/a > 1.020) had tendency to spall after the deposition cycle. Then, it is possible to evaluate the maximum content of niobia that can be added to the yttria doped zirconia coating without losses in its mechanical properties. Thus, through the graph of Figure 7, a coating with 8.7 mol % $YO_{1.5}$ (8 wt.% yttria) can be co-doped with up to 10 mol % $NbO_{2.5}$ (10.8 wt.% niobia).

Figure 8 shows the typical microstructure of EB-PVD ceramic coating, as seen by SEM on polished cross section. The ceramic layer shows color bands associated with chemical composition changes due to the differences in saturation vapor pressure of the individual components as function of the temperature and complex chemical interactions between them. For these reasons, the evaporation of alloys is a selective process, resulting in depletion and enrichment in the melt pool and, consequently, in the coating.

The results of EDS analysis performed on the ceramic coating cross section are summarized in Figure 9. The composition of the ceramic layer differs point-to-point, remarkable for the niobia concentration due to the difference in melting point and vapor pressure between niobia, zirconia and yttria. It is clear that compositional gradients can reduce the thermal stability due to differences in layers thermal expansion coefficients. Nevertheless, because of the high melting point of the ceramic, the liquid pool during evaporation is shallow in comparison with target volume, there is not sufficient liquid volume for high level of segregation and as the process is predominantly randonic, the influence in the thermal stability and in the x-ray data is not high.

The results of the theoretical density from Equation I is shown in Figure 10. As the niobia content increases, there is a tendency to reduction of the ceramic coatings theoretical density (R=-0,614); despite of bigger niobia atomic mass than yttria and zirconia.

The influence of niobia content on the bulk density of ceramic layer is shown in Figure11; there is a minimum at 5 mol % $NbO_{2.5}$.

The introduction of niobia in the zirconia crystalline lattice decreases the thermal conductivity through the scattering of phonons promoted by the differences in mass, ionic radius and chemical bonds between the dopant and host atom. Beyond this, the thermal conductivity is directly proportional to the theoretical density of the material. Thus, the reduction in the theoretical density, promoted by niobia addition, can denote lower thermal conductivity than the conventional zirconia-yttria coatings. Moreover, microstructural defects are obstacles against the through-thickness heat transfer propagation. The lesser bulk density observed in the 5 to 10 mol % $NbO_{2.5}$ coatings (Figure 11) probably is associated with a high level of porosity this, in turn, contributes with an additional reduction in the thermal conductivity of the yttria and niobia co-doped zirconia coatings.

In PVD coatings, the structure is a strong function of the ratio of the substrate temperature to the melting point of the material being deposited. Figure 12 shows a sequence of coatings fractured cross sections where the niobia content is changed; a columnar structure of the ceramic layer is evident and its diameter increases with niobia content.

Thermal stability at high temperature preliminary studies, using a method developed by Vasinonta et ali [28], and thermal properties determinations, using flash method [29], whose details will be discussed in a future paper, showed that 8 mol % yttria and 5 to 10 mol % niobia co-doped zirconia EB-PVD coatings exhibited the same level of thermal stability and smaller thermal conductivity than conventional yttria doped zirconia coatings.

4. Conclusions

Based on the analysis of the results, the following conclusions can be drawn:

This new ceramic system (yttria and niobia co-doped zirconia) allows attaining coatings with microstructure similar to the conventional yttria doped zirconia EB-PVD TBCs.

The results of XRD analysis performed on the surface of the ceramic coating samples show, as in conventional TBCs, only the nonequilibrium zirconia tetragonal phase for the chemical composition range studied. As the difference ($NbO_{2.5}$ - $YO_{1.5}$) mol % increases, the ratio c/a (tetragonality) increases.

Despite of the possibility to obtain monophasic coatings for all composition studied, only those with niobia less than 10 mol % were stable. Solid solutions become unstable as their tetragonality increases toward 1.020, which corresponds to the c/b axial ratio of monoclinic zirconia.

The ceramic coatings cross sections show color bands associated with chemical composition changes due to the differences in saturation vapor pressure of the individual components. Nevertheless, because of the small size of the liquid pool in comparison with target volume, the segregation is not so high.

The thermal conductivity is directly proportional to the theoretical density of the material. Thus, the reduction in the theoretical density, promoted by niobia addition, can denote lower thermal conductivity than the conventional yttria doped zirconia coatings.

There is a minimum bulk density value at 5 mol % $NbO_{2.5}$ and this can allows obtaining ceramic coatings with low thermal conductivity due to high level of porosity.

It is expected that the single-phase tetragonal niobia and yttria co-doped zirconia coatings will have lower thermal conductivity than conventional 6-8 mol % yttria stabilized zirconia coatings, the material conventionally used for thermal barrier coating with others advantages, e. g., phase stability at high temperatures, cyclic life, ageing behavior which may prove superior to those of conventional zirconia.

Acknowledgments

References

[1] Xu, H., Goug, S., Deng, L., Thin Solid Films, 334 (1998) 98-102.

[2] Schulz, U. et ali, Surf. Coat. Technol., 133-134 (2000) 40-48.

[3] Zhu, D. et ali, NASA/TM-2000-210238.

[4] Goward, G. W., Surf. Coat. Technol., 108-109 (1998) 73-79.

[5] Nicholls, J.R., Deakin, M.J., Rickerby, D. S., Wear, 233-235 (1999) 352-361.

[6] Czek, N. et ali, Surf. Coat. Technol., 113 (1999) 157-164.

[7] Hass, D.D., Thermal Barrier Coatings via Directed Vapour Deposition, Doctor Degree Thesis, University of Virginia, May, 2001.

[8] Almeida, D. S. et ali, Manufatura de Revestimentos como Forma de Barreira Térmica, Anais do Congresso Brasileiro de Engenharia e Ciência dos Materiais, Natal, 2002.

[9] Hillery, R.V.; Coatings for High-Temperature Structural Materials-Trends and Opportunities. Washington - D. C.: National Academy Press, 1996. 85 p.

[10] Mumm, D. R.; Evans, A. G., Spitsberg, I. T. Acta Materialia, 49 (2001) 2329-2340.

[11] Stöver, D.; Funke, C., Journal Materials Processing Technology, 92-93 (1999) 195-202.

[12] Leyens, C.; Schulz, U., Pint, B. A., Wright, I. G., Surf. Coat. Technol., 120-121 (1999) 68-77.

[13] Vyas, J.D. ; Choy, K. –L., Materials Science and Engineering, A277 (2000) 206-212.

[14] Evans, A. G.; He, M. Y., Hutchinson, J. W., Progress in Materials Science, 46 (2001) 249-271.

[15] Kim, D. J., J. Am. Ceramic Soc., 73[1] 115-20 (1990).

[16] Lehmann, H.; Pracht, G., Vassen, R., Stöver, D., J. Am. Ceramic Soc., 86[8],1138-44 (2003).

[17] Kim, D. J. e Tien, T. Y., J. Am. Ceramic Soc., 74[12]3061-65 (1991).

[18] Lee, D. Y., et ali, J. Materials Science Letters, 17 (1998) 185-187.

[19] Schulz; et ali, Aerospace Science and Technology, 7 (2003) 73-80.

[20] Raghavan, S. et ali, Acta Materialia, 49 (2001) 169-179.

[21] Li, P. and Chen, I-W., J. Am. Ceram. Soc., 77[5] 1281-88 (1994).

[22] Guo, X. and Wang, Z., J. European Ceramic Society, 18 (1998) 237-240.

[23] Roth, R. S.; Coughanour, L. W. Phase Diagrams for Ceramists. Columbus, OH: The American Ceramic Socity, 1964.

[24] Guo, H.; Bi, X., Gong, S., Xu, H., Scripta Materialia, n. 44 (2001) 683-687.

[25] Raghavan, S.; et ali., Scripta Materialia, 39 [8] (1998) 1119-1125.

[26] Lelait, L, Alpérine, S., Diot, C., Journal de Physique III, 3 (1993) 645-654.

[27] Bernier, J. S. et ali, ; Levan, G., Maniruzzaman, Md., Sisson, R. D., Bose, S., Surf. Coat. Technol., 95-99 (2003) 163-164.

[28] Vasinonta, A.; Beuth, J. L., Engineering Fracture Mechanics, 68 (2001) 843-860.

[29] Couto, P. et ali. Flash method standardization in Brazil for the measurement of solid thermophysical properties, Anais do congresso de Metrologia, Recife, Pernambuco, Brasil, 2003.
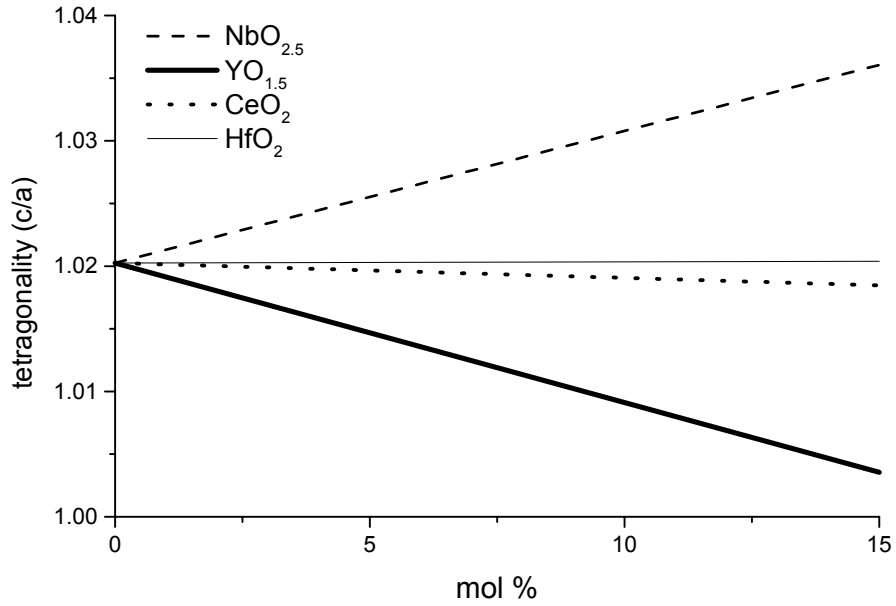
Figure 1: Influence of the alloying oxide in the c/a axial ratio of bulk zirconia based ceramics.
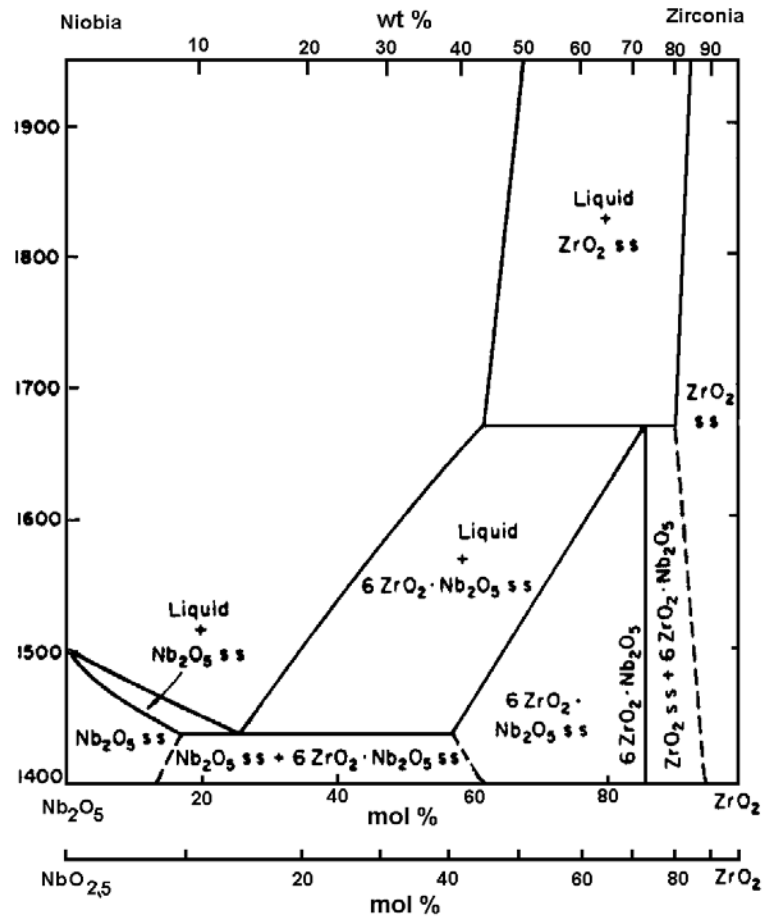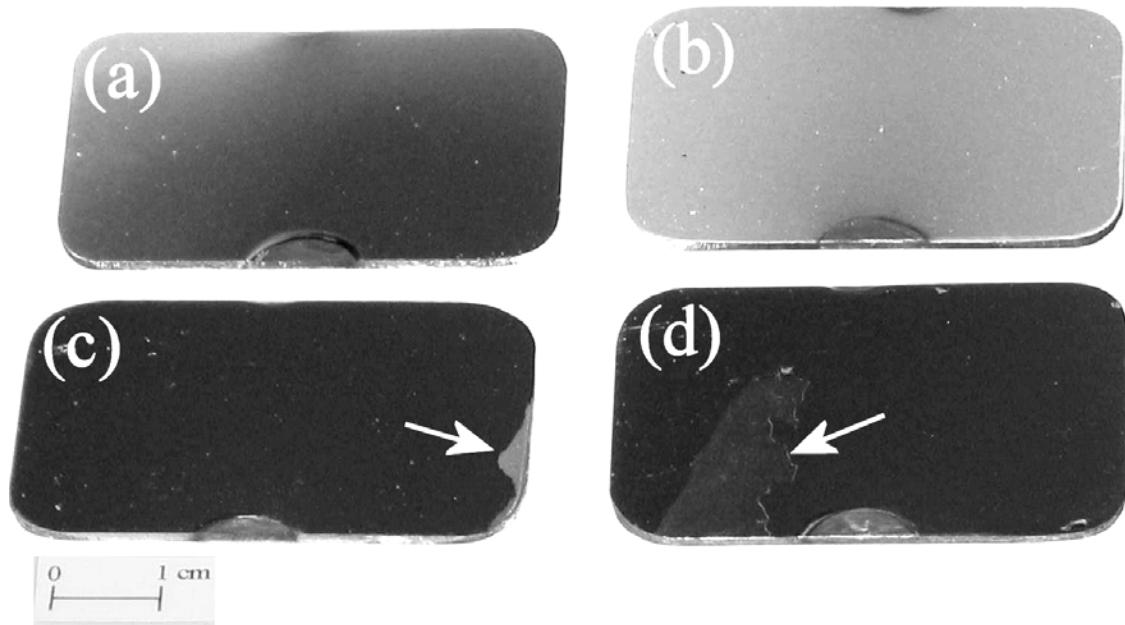

Figure 2: Nb_2O_5-ZrO_2 phase diagram.

Figure 3: Samples coated with zirconia, yttria plus (a) 0 mol %, (b) 5.1 mol %, (c) 10.9 mol % and (d) 14.5 mol % niobia. The arrows indicate spallations.
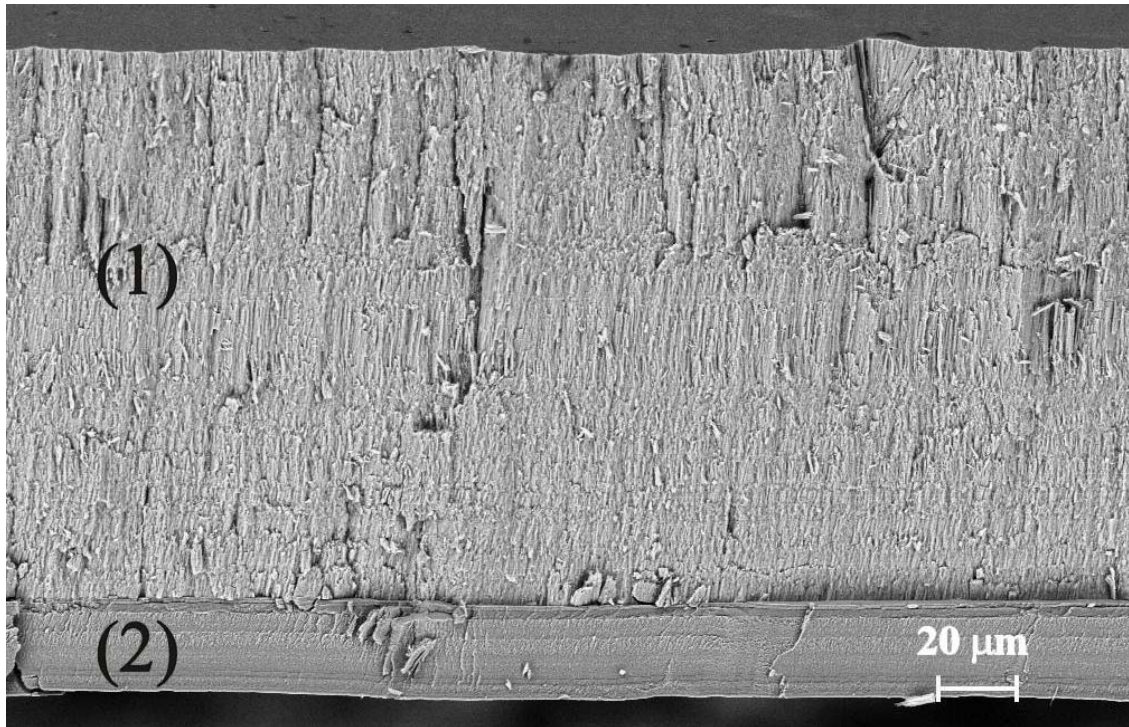

Figure 4: SEM (SE mode) of an EB-PVD thermal barrier coating fractured cross section; (1) ceramic layer; (2) metallic bond layer (sample 8).
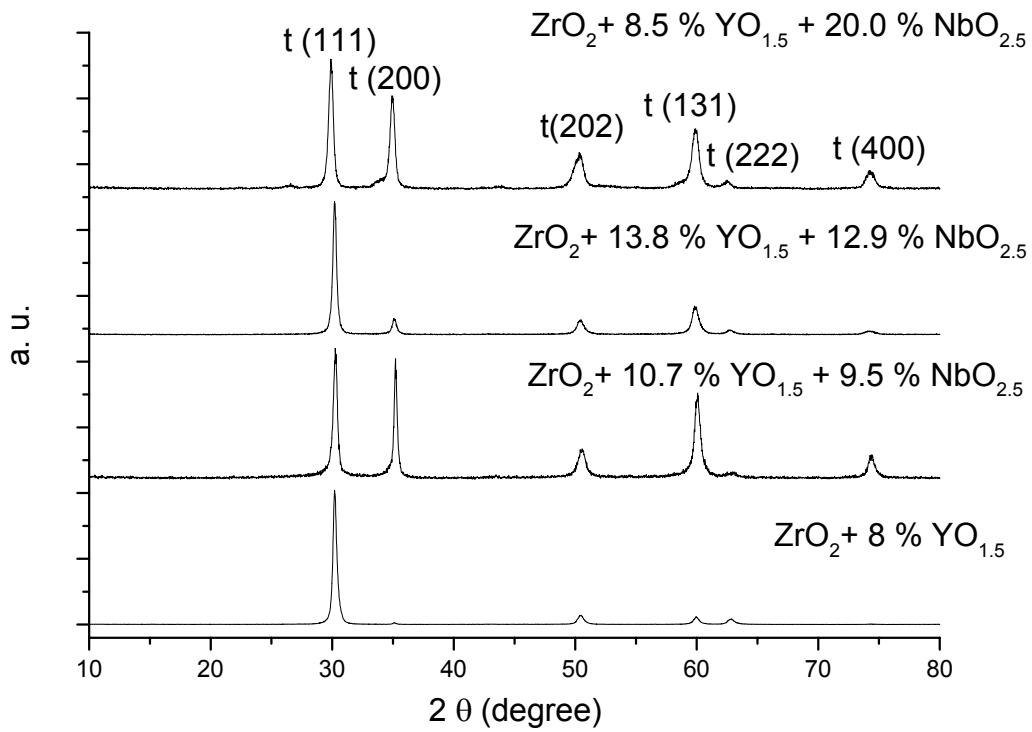
Figure 5: XRD in scanning mode of ceramic coatings with different niobia contents.
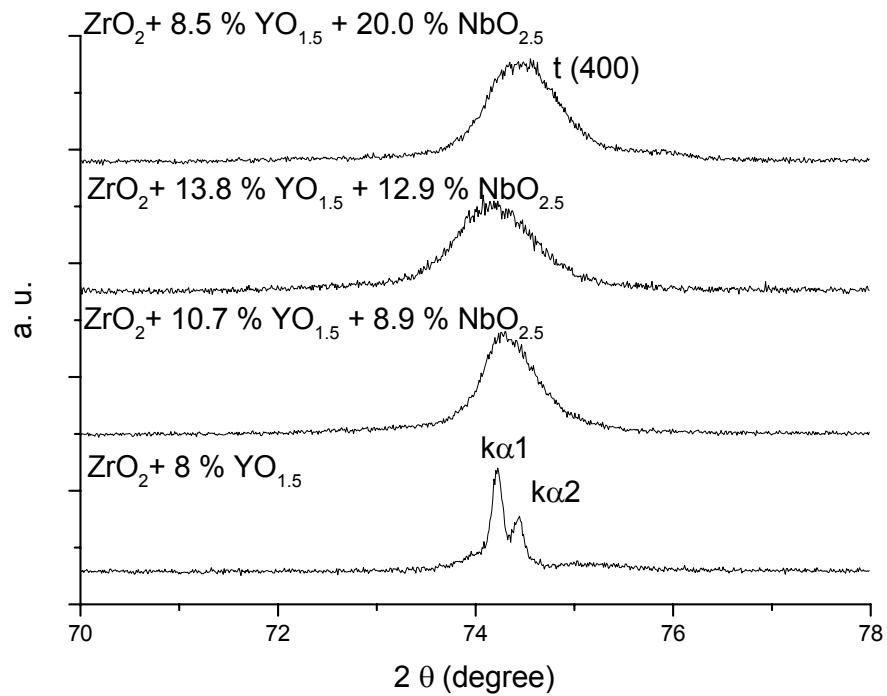
Figure 6: High angular resolution x-ray diffractograms for (400) region for the same coatings.
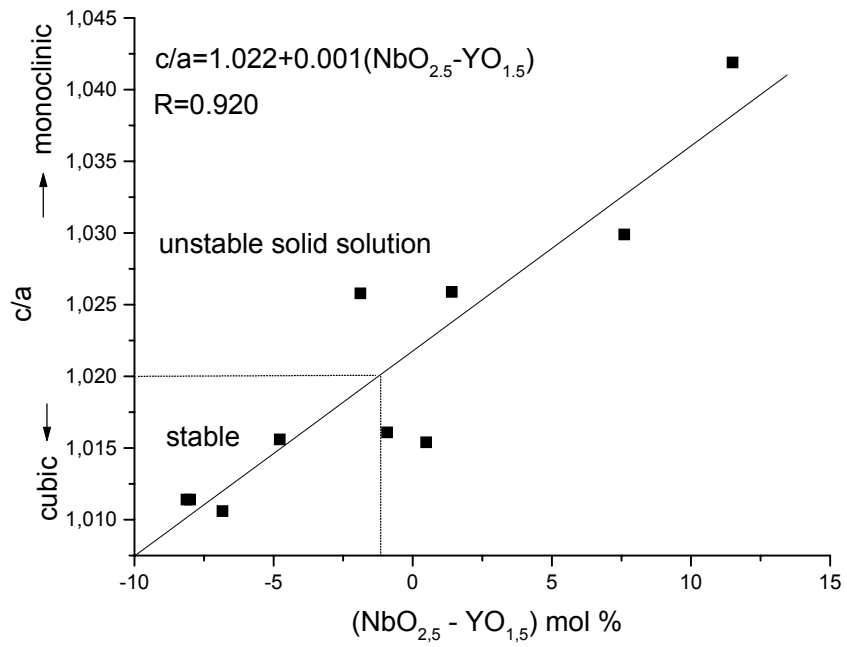
Figure 7: Relation between difference (NbO$_{2.5}$ -YO$_{1.5}$) mol % and tetragonality (c/a).
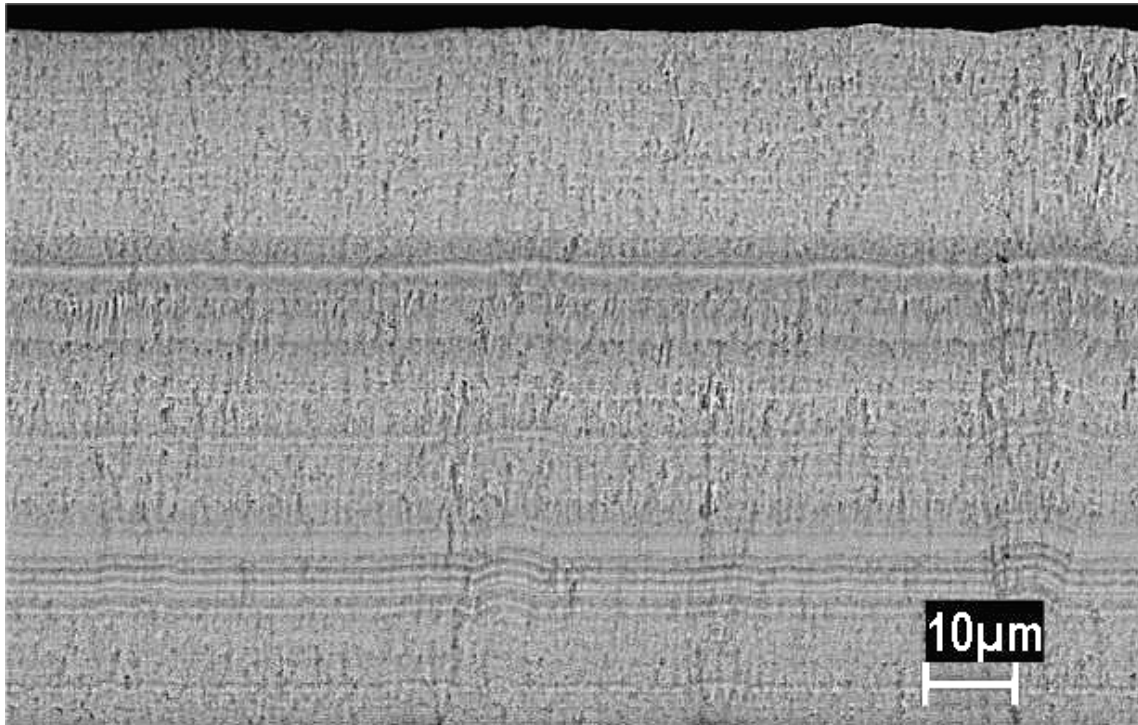
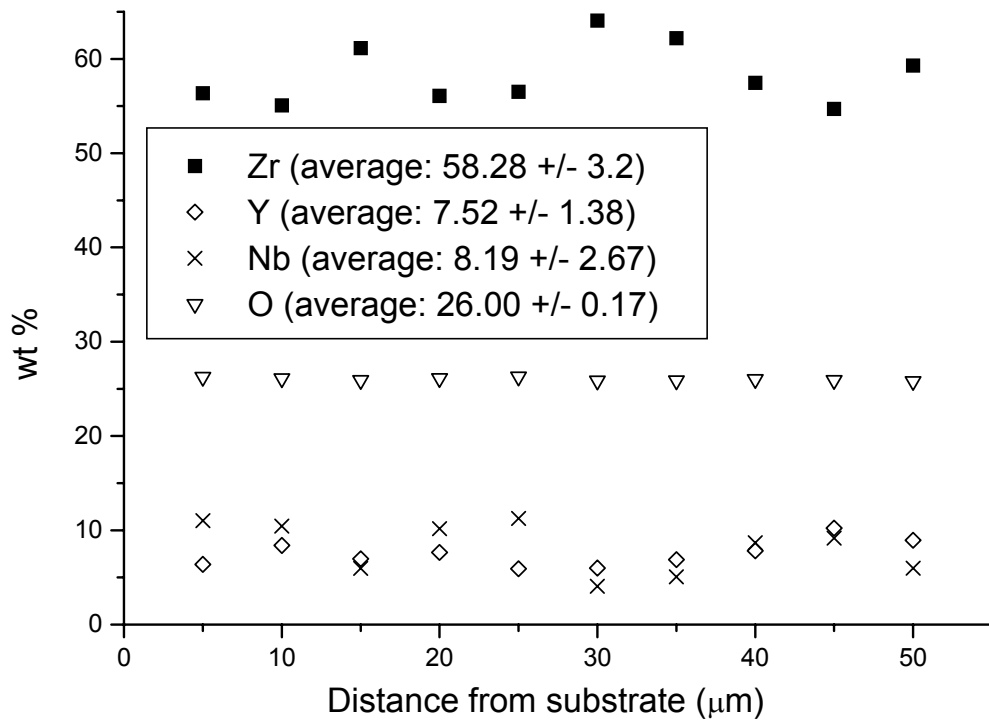Figure 8: SEM (BS mode) of an EB-PVD ceramic coating polished cross section (sample 8).

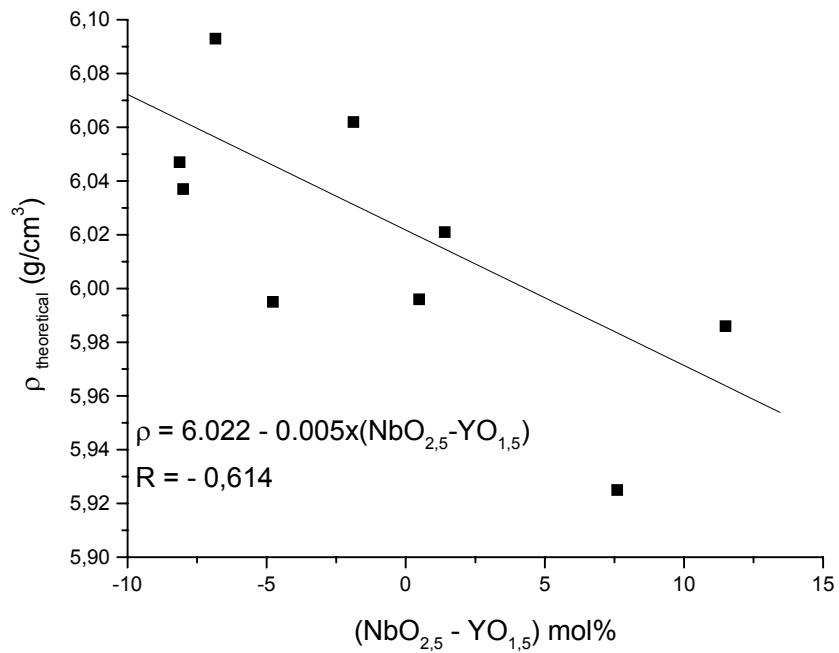Figure 9: EDS semi-quantitative analysis of ceramic layer (sample 8).

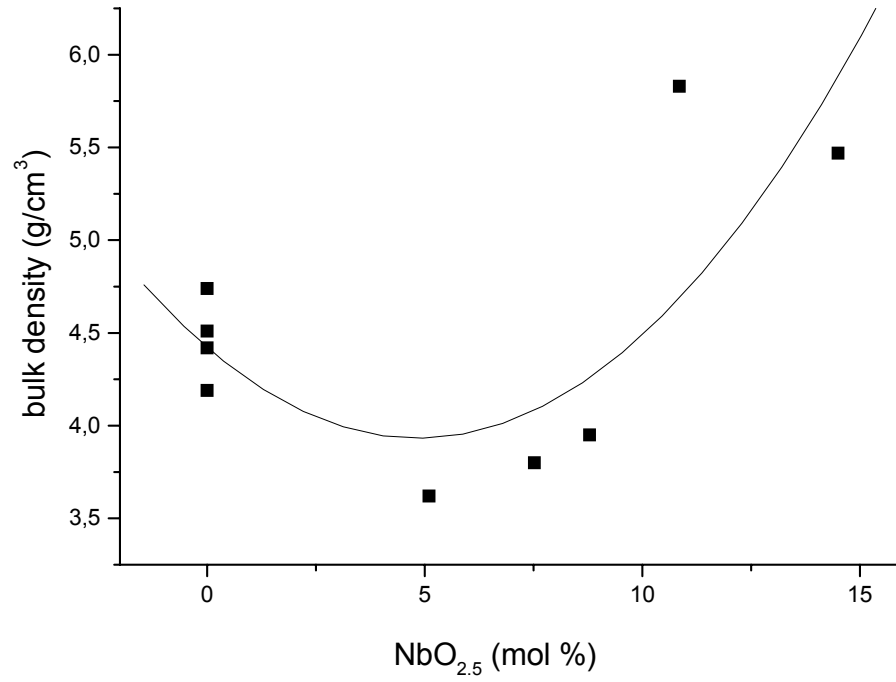Figure 10: Relation between the difference ($NbO_{2.5}$ -$YO_{1.5}$) mol % and theoretical density.
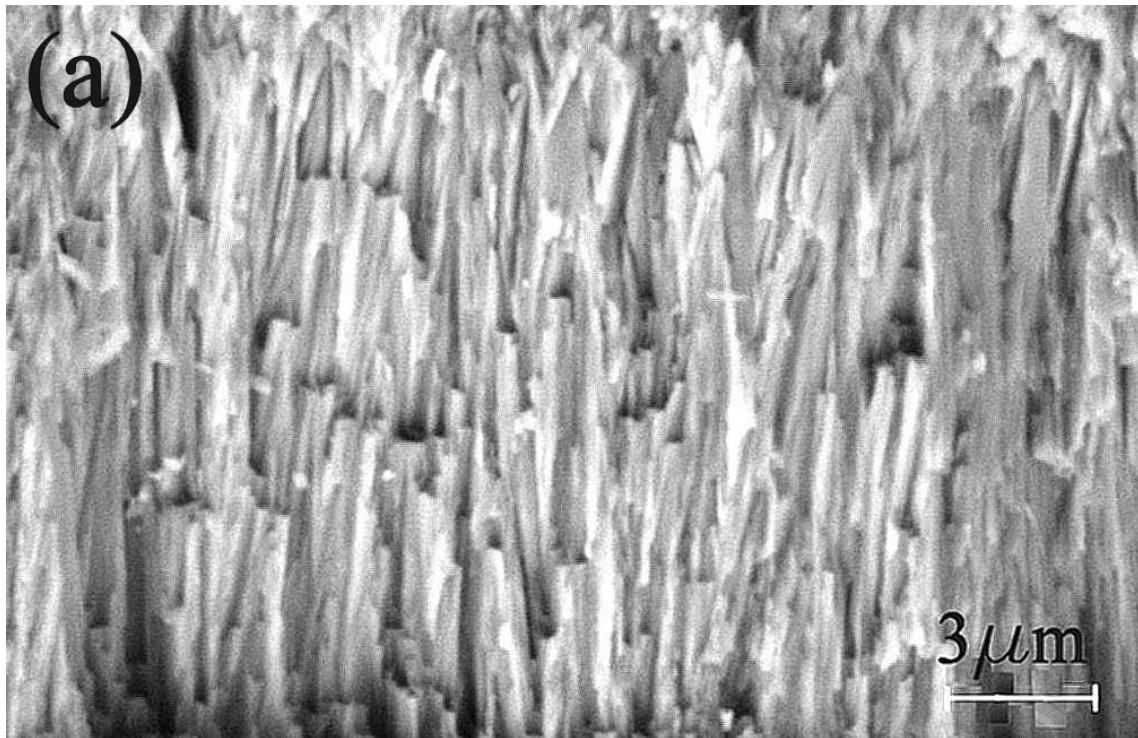
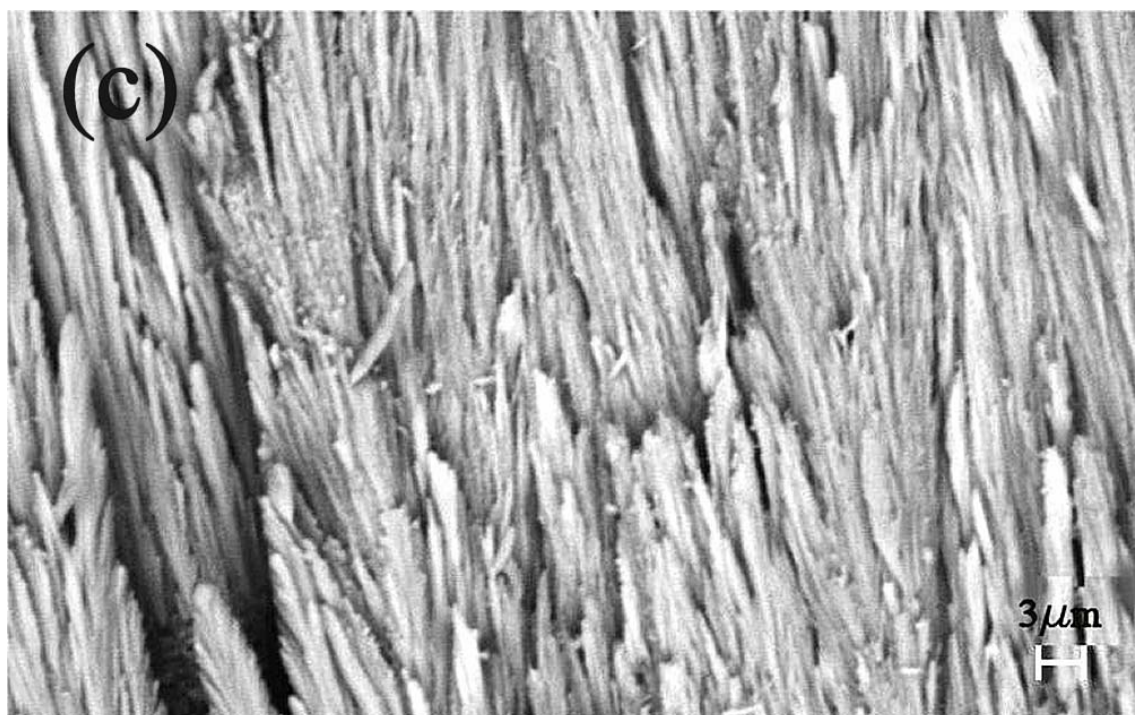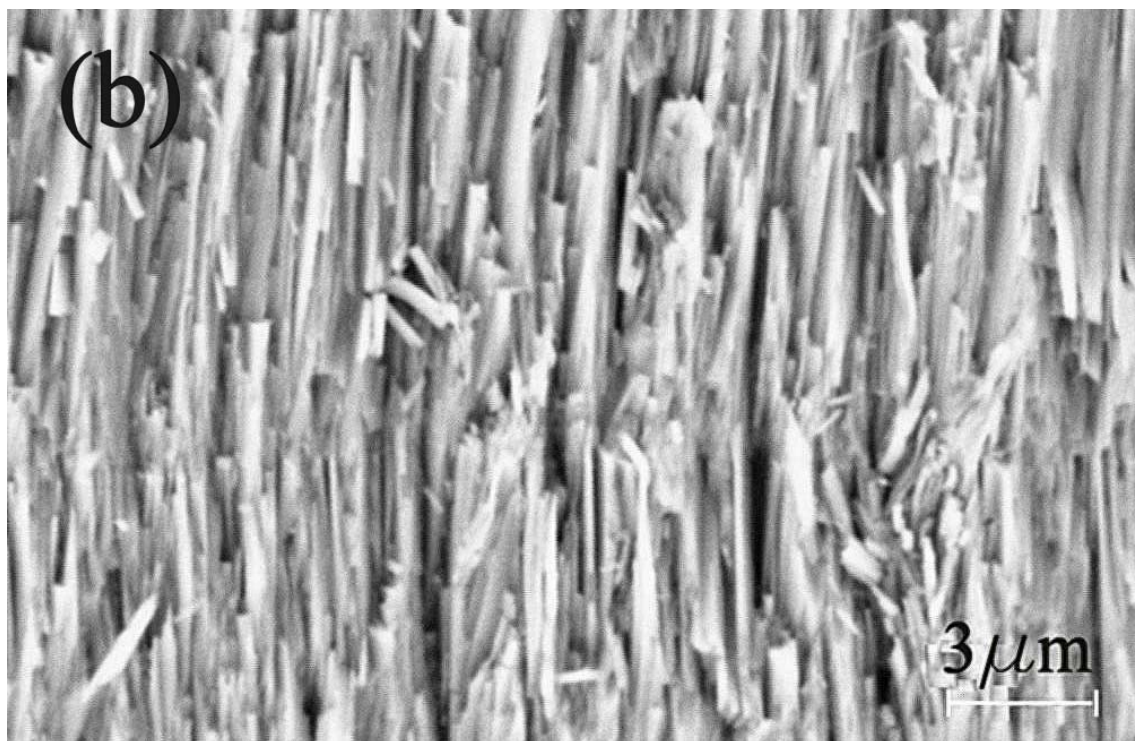Figure 11: Influence of niobia content in the bulk density of ceramic layer.

(a)

3 μm

Figure 12: SEM of EB-PVD ceramic coatings fractured cross section.
(a) Sample 1 (column diameter = 1.15 μm)
(b) Sample 6 (column diameter = 1.29 μm)
(c) Sample 11 (column diameter = 2.53 μm)

Table I: Chemical compositions and lattice parameters

Sample	Target					Coating				
	mol % ZrO_2	mol % $YO_{1.5}$	mol % $NbO_{2.5}$	mol %[1] $YO_{1.5}$	mol %[1] $NbO_{2.5}$	a	c	c/a	ρ (measured)	ρ (theor)[2]
1	91.3	8.7	0	8.00	0	5.1070	5.1650	1.0114	4.51	6.037
2	91.3	8.7	0	8.13	0	5.1040	5.1620	1.0114	4.74	6.047
3	91.3	8.7	0	6.84	0	5.0950	5.1490	1.0106	4.42	6.093
4	91.3	8.7	0	4.78	0	5.1170	5.1970	1.0156	4.19	5.995
5	87.0	8.0	5.0	5.13	5.10	-	-	-	3.62	-
6	82.0	8.7	9.3	6.12	7.52	5.1000	5.2320	1.0259	3.80	6.021
7	80.0	10.0	10.0	10.67	8.79	5.0840	5.2150	1.0258	3.95	6.062
8	77.2	8.8	14.0	10.37	10.85	5.1240	5.2030	1.0154	5.83	5.996
9	74.9	11.1	14.0	13.79	12.87	5.0960	5.1780	1.0161	-	6.104
10	72.7	9.1	18.2	8.53	20.02	5.1050	5.3190	1.0419	-	5.986
11	72.5	8.8	18.7	10.40	14.50	5.1240	5.2770	1.0299	5.47	5.925

[1] from EDS analysis on ceramic coating cross section.

[2] ρ_{theor} – Theoretical density using Equation 1.